

Strongly correlated Fermi–Bose mixtures in disordered optical lattices

L Sanchez-Palencia¹, V Ahufinger², A Kantian³, J Zakrzewski⁴,
A Sanpera⁵ and M Lewenstein^{6,7}

¹ Laboratoire Charles Fabry de l'Institut d'Optique, CNRS and Université Paris-Sud XI, Bât 503, Centre scientifique, F-91403 Orsay Cedex, France

² ICREA and Grup d'òptica, Departament de Física, Universitat Autònoma de Barcelona, E-08193 Belaterra (Barcelona), Spain

³ Institut für Theoretische Physik, Universität Innsbruck, A-6020 Innsbruck, Austria

⁴ Instytut Fizyki imienia Mariana Smoluchowskiego i Centrum Badań Układów Złożonych imienia Marka Kaca, Uniwersytet Jagielloński, ulica Reymonta 4, PL-30-059 Kraków, Poland

⁵ ICREA and Grup de Física Teòrica, Departament de Física, Universitat Autònoma de Barcelona, E-08193 Belaterra (Barcelona), Spain

⁶ ICREA and ICFO-Institut de Ciències Fotòniques, Parc Mediterrani de la Tecnologia, E-08860 Castelldefels (Barcelona), Spain

⁷ Institut für Theoretische Physik, Universität Hannover, D-30167 Hannover, Germany

E-mail: laurent.sanchez-palencia@iota.u-psud.fr

Received 30 November 2005, in final form 8 December 2005

Published 2 May 2006

Online at stacks.iop.org/JPhysB/39/S121

Abstract

We investigate theoretically the low-temperature physics of a two-component ultracold mixture of bosons and fermions in disordered optical lattices. We focus on the strongly correlated regime. We show that, under specific conditions, composite fermions, made of one fermion plus one bosonic hole, form. The composite picture is used to derive an effective Hamiltonian whose parameters can be controlled via the boson–boson and the boson–fermion interactions, the tunnelling terms and the inhomogeneities. We finally investigate the quantum phase diagram of the composite fermions and show that it corresponds to the formation of Fermi glasses, spin glasses and quantum percolation regimes.

(Some figures in this article are in colour only in the electronic version)

1. Introduction to disordered quantum systems

1.1. From condensed matter physics to ultracold atomic gases

Quantum disordered systems is a very active research field in condensed matter physics (CM) initiated by the work by Anderson [1] who first pointed out that quenched (i.e. time-independent) disorder can dramatically change the properties of a quantum system compared

to its long-range ordered counterpart. Hence, disorder plays a central role in modern solid state physics as it can significantly alter electronic normal conductivity [2], superconductivity [3] and the magnetic [4, 5] properties of dirty alloys.

It is by now clear that studying disordered systems is comparable to opening the *Pandora box*. On the one hand, disorder introduces a list of non-negligible difficulties. First, averaging over disorder usually turns out to be a complex task that requires either original methods such as the replica trick [4] and supersymmetry [6] or numerical computations using huge samples or a large number of repetitions with different configurations. Second, the possible existence of a huge number of excited states with infinitely small excitation energies leads to complex quantum phases such as Bose glasses [7] or spin glasses [4]. Third, the interplay of kinetic energy, particle–particle interactions and disorder is usually a non-trivial problem [8] which is still challenging. On the other hand, disorder leads to an extraordinary variety of physical phenomena such as, for example, Anderson localization [1], quantum percolation [9] or quantum frustration [10].

Studies of quantum disorder in CM have several limitations. First, the disorder cannot be controlled as it is fixed by the specific realization of the sample. In particular, one cannot switch adiabatically from one configuration to another. Second, the particles are fermions (electrons) and the inter-particle interaction corresponds to the Coulomb long-range potential. Third, theoretical studies rely on toy models and experiments do not provide control parameters. Thus, it would be highly desirable to consider new kinds of disordered quantum systems. As shown in this work and also discussed in other papers [11, 12], one exciting possibility is that of ultracold atomic gases where these problems can be revisited with unique parameters control and measurement possibilities.

1.2. Ultracold atomic gases

Following the recent progress in cooling and trapping of neutral atoms [13], dilute atomic Bose–Einstein condensates (BEC) [14], degenerate Fermi gases (DFG) [15] and mixtures of both [16] are now currently produced at the laboratory. In these systems almost all parameters prove to be highly controllable [17]: (i) using standard techniques, one can easily control the trapping potential, the size, the density and the temperature of the atomic gas. (ii) Due to the strong dilution, the contact interactions are usually small and can be computed *ab initio*. In addition, their sign and strength can be controlled using Feshbach resonances [18]. (iii) Quantum statistics is also a degree of freedom as one can use bosons or fermions. (iv) Finally, inhomogeneous trapping potentials can be designed almost at will using standard optical techniques. In particular, periodic potentials (optical lattices) with no defect nor phonons can be designed in a wide variety of geometries [19]. Controlled disordered [20] or quasi-disordered [21, 22] potentials can also be optically produced opening new possibilities. Hence, equilibrium and transport properties of interacting Bose–Einstein condensates in random potentials have been investigated in recent experiments [23–25].

In recent works [12, 26], we have shown that Fermi–Bose mixtures in an optical lattice with diagonal (i.e. with random on-site energy) randomness constitute a case study of quantum disordered systems. In the strongly correlated regime (strong interactions), the dynamics reduces to a universal effective Hamiltonian whose parameters can be controlled through the boson–boson and fermion–boson interactions, or the depth of the periodic and disordered potentials. It results in a rich quantum phase diagram ranging from Fermi glasses and Fermi Anderson localization to quantum spin glasses and quantum percolation [12].

This paper reviews our works on strongly correlated Fermi–Bose mixtures in disordered optical lattices. It further details the results discussed in [12]. In [26], we have presented

a complete study of the system and discussed a wide variety of cases, including several composite types and quantum phases. As in such a rich system, completeness competes with conciseness, we think that a shorter review would be useful for non-specialist readers. It is the aim of this paper to provide such a concise review of our findings. We have thus chosen to restrict the present analysis to a specific case that proves to be nonetheless paradigmatic but also one of the richest ones. For more details, the interested reader should refer to [26].

This paper is organized as follows. In section 2, we introduce the model describing the considered system (2.1) and the composite fermions formalism that leads to the effective Hamiltonian (2.2) and (2.3). Section 3 shows the results for the non-disordered and weakly disordered lattices and in section 4 the strong disorder limit, the spin glass limit, is discussed. Finally, we summarize and discuss our results in section 5.

2. Strongly correlated composite fermions in inhomogeneous optical lattices

2.1. The Fermi–Bose Hubbard Hamiltonian

Consider a mixture of ultracold bosons (b) and spinless (or spin-polarized) fermions (f) trapped in an optical lattice. In addition, the mixture is subjected to on-site inhomogeneities consisting in a harmonic confining potential and/or in a diagonal disorder. Eventually, the periodic potential and the inhomogeneities are different for the bosons and the fermions. However, we assume that the lattices for the two species have the same periodicity. The lattice sites are indexed by i and are thus the same for the fermions and the bosons. In all cases considered below, the temperature is assumed to be low enough and the potential wells deep enough so that only quantum states in the fundamental Bloch bands for both the bosons and the fermions are populated. Note that this requires that the filling factor for fermions ρ_f is smaller than 1 i.e. the total number of fermions N_f is smaller than the total number of lattice sites N .

We use the Wannier basis of the fundamental Bloch band which corresponds to wavefunctions well localized in each lattice site [27] for both the bosons and the fermions. This basis is particularly well suited for the strongly correlated regime that is investigated here [28]. Then, the second quantization Hamiltonian reduces to the Fermi–Bose Hubbard (FBH) model [3, 5, 29]:

$$H_{\text{FBH}} = - \sum_{\langle ij \rangle} \left[J_b b_i^\dagger b_j + J_f f_i^\dagger f_j + \text{h.c.} \right] + \sum_i \left[\frac{V}{2} n_i (n_i - 1) + U n_i m_i \right] + \sum_i \left[-\mu_i^b n_i - \mu_i^f m_i \right], \quad (1)$$

where b_i and f_i are bosonic and fermionic annihilation operators of a particle in the i th site and $n_i = b_i^\dagger b_i$, $m_i = f_i^\dagger f_i$ are the corresponding on-site number operators. The FBH model describes (i) nearest-neighbour boson (fermion) hopping, with an associated negative energy, $-J_b$ ($-J_f$); (ii) on-site boson–boson interactions with an energy V , which is supposed to be positive (i.e. repulsive) in the remainder of the paper; (iii) on-site boson–fermion interactions with an energy U , which is positive (negative) for repulsive (attractive) interactions; (iv) on-site energy due to interactions with a possibly inhomogeneous potential, with energies $-\mu_i^b$ and $-\mu_i^f$. Eventually, $-\mu_i^b$ and $-\mu_i^f$ also contain the chemical potentials in the grand canonical description.

In the following, we investigate the properties of the strong coupling regime, i.e. $V, U \gg J_{b,f}$ and we derive a one-species effective Hamiltonian using a perturbative development up to second order in $J_{b,f}/V$.

2.2. Zeroth-order perturbation: formation of fermion composites

In the limit of a vanishing hopping ($J_b = J_f = 0$) with the finite repulsive boson–boson interaction V , and in the absence of interactions between bosons and fermions ($U = 0$), the bosons are pinned in the lattice sites with exactly $\tilde{n}_i = \lceil \tilde{\mu}_i^b \rceil + 1$ bosons per site, where $\tilde{\mu}^b = \mu^b/V$ and $\lceil x \rceil$ denotes the integer part of x . For simplicity, we assume $\tilde{n}_i = 1$ for all sites so that the boson system is in the Mott insulator (MI) phase with 1 boson per site. In contrast, the fermions can be in any set of Wannier states, since for a vanishing tunnelling, the energy of the system does not depend on the distribution of the fermions in different lattice sites for the homogeneous optical lattice and will be very similar for the different repartitions of fermions in the case of small disorder.

Assume now that the boson–fermion interaction is turned on positive ($U > 0$) and define $\alpha = U/V$. The presence of a fermion in site i may expel $s = 0$ or 1 boson depending on the interaction strength. The on-site energy gain in expelling s boson from site i is $\Delta E_i = \frac{V}{2}s(s-1) - Us + \mu_i^b s$. Minimizing ΔE_i versus s , we find that $s = \lceil \alpha - \tilde{\mu}_i^b \rceil + 1$ that we assume to be 1 in all sites. Within the occupation number basis, excitations correspond to having 1 boson in a site with a fermion, instead of 0 boson and, therefore, the corresponding excitation energy is $\sim U$. In the following, we assume that the temperature is smaller than U so that the populations of the above-mentioned excitations can be neglected.

Summarizing the above discussion, we have assumed that $0 < \mu_i^b < V$ (so that $\tilde{n}_i = 1$), $U - V < \mu_i^b < U$ (so that in the lowest energy states, each lattice site is populated by either one boson or one fermion but never 0 or 2 particles), and $k_B T < U$ (so that only these lowest energy states are significantly populated). The physics of our Fermi–Bose mixture can thus be regarded as the one of composite particles made of one fermion plus one bosonic hole. Note that the bosonic hole is created because the initially present boson is expelled from the site by the fermion, due to the repulsive interactions between bosons and fermions. Within the picture of composites, a lattice site is either populated by one composite (i.e. by one fermion plus bosonic hole) or free of composite (i.e. populated by one boson). In particular, the vacuum state corresponds to the MI phase with 1 boson per site. The annihilation and creation operators of the composites are [30]

$$F_i = b_i^\dagger f_i \mathcal{P} \quad (2)$$

$$F_i^\dagger = \mathcal{P} f_i^\dagger b_i, \quad (3)$$

where \mathcal{P} is the projector onto the sub-Hilbert space of the composites. It is straightforward to show that F_i and F_i^\dagger are fermionic operators.

2.3. Second-order perturbation: effective Hamiltonian

The sub-Hilbert space of the composites is $[N!/(N_f!(N - N_f)!)]$ -dimensional, a number that corresponds to the number of possibilities of distributing the N_f fermions into the N lattice sites. We assume now that the tunnelling rates J_b and J_f are small but finite. For weak enough disorder, one can assume site-independent tunnelling rates for bosons and fermions [11]. Using the second-order projection perturbation theory [31], we derive an effective Hamiltonian for the fermionic composites by means of a unitary transform applied to the total Hamiltonian (1). The general expression of the effective Hamiltonian can be written as

$$\begin{aligned} \langle \text{out} | H_{\text{eff}} | \text{in} \rangle &= \langle \text{out} | H_0 | \text{in} \rangle + \langle \text{out} | \mathcal{P} H_{\text{int}} \mathcal{P} | \text{in} \rangle - \frac{1}{2} \langle \text{out} | \mathcal{P} H_{\text{int}} \mathcal{Q} \\ &\times \left[\frac{1}{H_0 - E_{\text{in}}} + \frac{1}{H_0 - E_{\text{out}}} \right] \mathcal{Q} H_{\text{int}} \mathcal{P} | \text{in} \rangle, \end{aligned} \quad (4)$$

where $\mathcal{Q} = 1 - \mathcal{P}$ is the complement of the projection operator \mathcal{P} . As the second-order theory can only connect states that differ on one set of two adjacent sites, H_{eff} can only contain nearest-neighbour hopping and interactions as well as on-site energies $\bar{\mu}_i$ [12]:

$$H_{\text{eff}} = \sum_{(i,j)} [-d_{i,j} F_i^\dagger F_j + \text{h.c.}] + \sum_{(i,j)} K_{i,j} M_i M_j + \sum_i \bar{\mu}_i M_i, \quad (5)$$

where F_i and F_i^\dagger are defined in equations (2) and (3) and $M_i = F_i^\dagger F_i$ is the composite number operator in the lattice site i . Although the general form of Hamiltonian (5) is universal for all types of composites, the explicit calculation of the coefficients $d_{i,j}$, $K_{i,j}$ and $\bar{\mu}_i$ depends on the concrete type of composites that can be created for different values and sign of alpha [26]. The nearest-neighbour hopping for the composites is described by $-d_{i,j}$ and the nearest-neighbour composite–composite interaction is given by $K_{i,j}$, which may be repulsive (>0) or attractive (<0). This effective model is equivalent to that of spinless interacting fermions [3].

In the situation under consideration, each site contains either one boson or one fermion. Therefore, a fermion jump from site i to site j can only occur if the boson that was initially in site j jumps back to site i into the hole the fermion leaves behind. Therefore, the number operator for fermions and bosons is related to the number operator of composites, i.e. $M_i = m_i = 1 - n_i$. From equation (4), we find

$$d_{ij} = \frac{J_b J_f}{V} \left(\frac{\alpha}{\alpha^2 - (\Delta_{ij}^b)^2} + \frac{\alpha}{\alpha^2 - (\Delta_{ij}^f)^2} \right) \quad (6)$$

$$K_{ij} = -\frac{J_b^2}{V} \left(\frac{4}{1 - (\Delta_{ij}^b)^2} - \frac{2\alpha}{\alpha^2 - (\Delta_{ij}^b)^2} \right) - \frac{J_f^2}{V} \left(\frac{2\alpha}{\alpha^2 - (\Delta_{ij}^f)^2} \right) \quad (7)$$

$$\bar{\mu}_i = \mu_i^b - \mu_i^f + \frac{J_b^2}{V} \sum_{(i,j)} \left[\frac{4}{1 - (\Delta_{ij}^b)^2} - \frac{1}{\alpha - \Delta_{ij}^b} \right] - \frac{J_f^2}{V} \sum_{(i,j)} \left[\frac{1}{\alpha + \Delta_{ij}^f} \right], \quad (8)$$

with $\Delta_{ij}^{f,b} = \tilde{\mu}_i^{f,b} - \tilde{\mu}_j^{f,b}$ measuring the inhomogeneity of the lattice sites. Here, (i, j) represents all sites j adjacent to site i . The coupling parameters in Hamiltonian (5) depend on all parameters ($J_b, J_f, U, V, \mu_i^b, \mu_i^f$) of the FBH model (1) in a complex fashion. For example, the hopping amplitudes $d_{i,j}$ depend on disorder but always remain positive. In contrast, the interaction term $K_{i,j}$ can be positive or negative. All terms $d_{i,j}, K_{i,j}, \bar{\mu}_i$ are random due to the inhomogeneous on-site energies μ_i^b and μ_i^f of the bosons and the fermions, respectively. It is thus clear that the *qualitative character of interactions* may be controlled by the inhomogeneities [12].

For example, consider the case where disorder only applies to the bosons ($\mu_i^f = \text{cst}$, uniform)⁸. The corresponding coupling parameters are plotted in figure 1. As mentioned above, the hopping amplitudes d_{ij} are always positive, although may vary quite significantly with disorder, especially when $\Delta_{ij}^b \simeq \alpha$. As shown in figure 1, for $\alpha > 1$, $K_{ij} \leq 0$ and we deal with attractive (although random) interactions. For $\alpha < 1$, $K_{ij} \geq 0$ and the interactions between composites are repulsive. For $\alpha < 1$, but close to 1, K_{ij} might take positive or negative values for Δ_{ij}^b small or $\Delta_{ij}^b \simeq \alpha$.

In the following two sections, we investigate the ground-state properties of the Fermi–Bose mixture (or equivalently that of the fermion composites) in the presence of diagonal disorder. We distinguish two limiting cases. The first corresponds to small disorder while the second corresponds to $\Delta_{i,j}^{(b)} \simeq \alpha$ that interestingly maps to a spin glass problem.

⁸ This situation can be realized experimentally by, for example, choosing the frequency of the laser field that creates the lattices between two atomic transitions (see [32]).

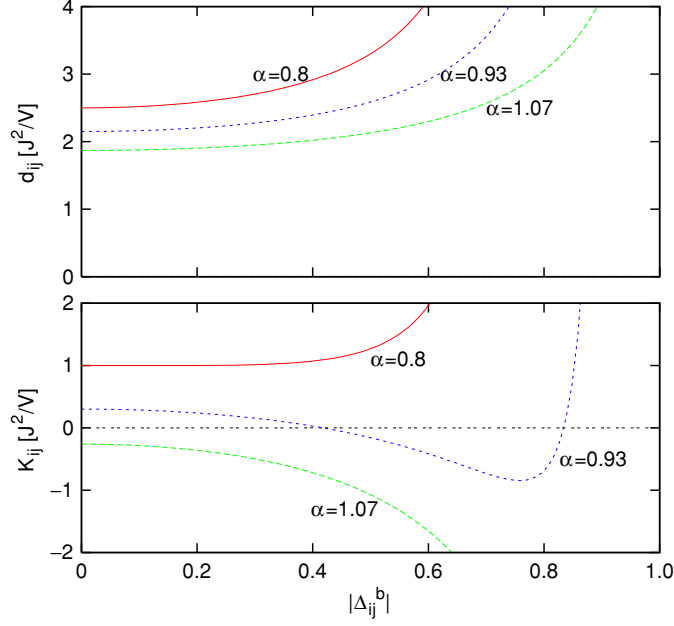


Figure 1. Tunnelling, d_{ij} , and nearest-neighbour interactions K_{ij} between the fermion composites as a function of the disorder of bosons Δ_{ij}^b for various boson–fermion interactions α . The disorder for fermions is assumed to vanish here ($\mu_i^f = 0$).

3. Quantum phase diagrams of Fermi–Bose mixtures in weakly disordered optical lattices

The first limiting case corresponding to weak disorder ($\Delta_{i,j}^{(f,b)} \ll 1, \alpha$) is investigated in this section. For the sake of simplicity, we use $J_b = J_f = J$. In this limit, the contributions of the inhomogeneities $\Delta_{ij}^{b,f}$ to the tunnelling d_{ij} and to the interaction K_{ij} terms in the effective composite Hamiltonian (5) can be neglected ($d_{ij} \simeq d$ and $K_{ij} \simeq K$) and we keep only the leading disorder contribution in $\bar{\mu}_i$ (the first term in equation (8)). Note that the latter contribution is particularly relevant in 1D and 2D leading to Anderson localization of single particles [33]. We will first describe the non-disordered case and then will discuss the effect of weak disorder.

The analysis reported below is supported by mean-field numerical calculations (for details about the numerical method, see [26]). We consider a 2D optical lattice with $N = 100$ sites with $N_b = 60$ bosons, $N_f = 40$ fermions and $J_b/V = J_f/V = 0.02$ to compute the ground state of the system in the presence of a very shallow harmonic trapping potential ($\mu_i^{b,f} = \omega^{b,f} \times l(i)^2$, where $l(i)$ is the distance from site i to the centre in cell size units) with eventually different amplitudes for bosons and fermions. This simulates optical or magnetic trapping which turns out to be hardly avoidable in current experiments on ultracold atoms. In addition, it breaks the equivalence of all lattice sites and makes more obvious the different phases that one can achieve (see below). In the numerics, we have used $\omega^b = 10^{-7}$ and $\omega^f = 5 \times 10^{-7}$.

In the absence of interactions between the bosons and the fermions ($\alpha = 0$), the bosons are well inside the MI phase with $\bar{n} = 1$ boson per site in the centre of the trap [7, 28]. Besides,

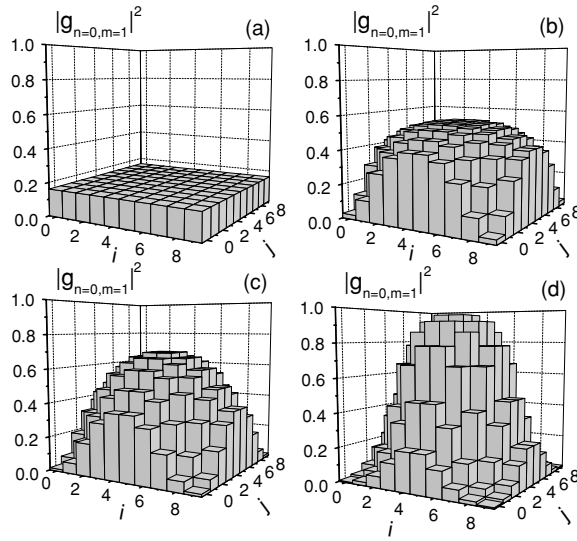


Figure 2. Local on-site probability of finding one fermion and zero boson at each lattice site for the $N = 100$ lattice sites in a Fermi–Bose mixture with $N_b = 60$, $N_f = 40$, $J_b/V = J_f/V = 0.02$ and in the presence of harmonic traps for bosons and fermions characterized by $\omega_b = 10^{-7}$ and $\omega_f = 5 \times 10^{-7}$, respectively. The interaction between fermions and bosons is (a) $\alpha = 0$ (independent bosonic MI and Fermi gas), (b) $\alpha = 0.5$ (Fermi liquid), (c) $\alpha = 1$ (ideal Fermi gas) and (d) $\alpha = 10$ (fermionic insulator domain).

the non-interacting fermions are delocalized and due to the very small value of ω^f they do not feel significantly the confining trap as shown in figure 2(a).

3.1. Quantum phases in non-disordered optical lattices

In the absence of disorder, the physics of the Fermi–Bose mixture is mainly determined by the ratio K/d and the sign of K where K and d are site-independent parameters. Once the fermion composites are created ($\alpha > \tilde{\mu}^b$, see section 2.2), we have $K/d = -2(\alpha - 1)$ as a result of equations (6) and (7) with $J_b = J_f = J$ and $\Delta_{ij} = 0$. We now discuss the quantum phases that are accessible depending on the control parameter α .⁹

For $\tilde{\mu}^b < \alpha < 1$, the interactions between composite fermions are repulsive and of the same order of magnitude as the tunnelling ($K \sim d$). Therefore, the system enters an interacting *Fermi liquid* quantum phase (see figure 2(b)). The fermions are delocalized over the entire lattice but populate preferably the centre of the confining trap. Small repulsive composite interactions tend to flatten the density profile compared to that of non-interacting composites (see figure 2 and the text below).

For $\alpha \simeq 1$, although the interactions between the bosons and the fermions are large, the interactions between the fermion composites vanish and the system shows up properties of an *ideal Fermi gas* (see figure 2(c)). Again, the fermions are delocalized and their distribution follows the harmonic confinement.

Growing further the repulsive interactions between bosons and fermions, the interactions between the fermion composites become attractive. For $1 < \alpha < 2$, one expects the system to be a weakly interacting *superfluid*, whereas for $\alpha > 2$ a *fermionic insulator domain* phase is

⁹ Note that, as discussed in section 2.2, we restrict the analysis to the case $\mu_i^b < \alpha < 1 + \mu_i^b$.

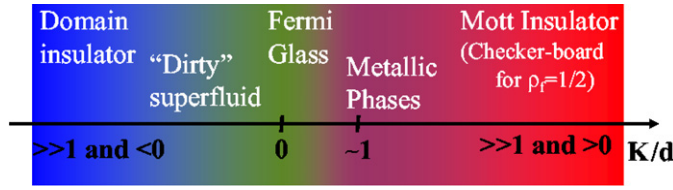


Figure 3. Schematic phase diagram of fermionic composites for small disorder ($\Delta_{ij}^b \ll 1, \alpha$) as a function of the ratio of the nearest-neighbour interactions and tunnelling of the composites (K/d).

predicted (see figure 2(d)). In this case, the fermions are pinned in the lattice sites. They tend to merge because of site-to-site attractive interactions and populate the centre of the trap.

Note that contrary to the bare fermions, the composite fermions are significantly affected by the harmonic trapping potential. This is because the coupling parameters of the composite effective Hamiltonian (5) are much smaller than the coupling parameters of the bare fermion–boson Hubbard Hamiltonian (1). Therefore the harmonic potential is able to compete with tunnelling and interactions for the composites [26].

3.2. Quantum phases in disordered optical lattices

We now assume that small on-site inhomogeneities are present and investigate the effect of disorder on the quantum phase diagram of the system depending on the parameters of the effective Hamiltonian (5). Figure 3 shows a schematic representation of expected disordered phases of the fermionic composites for small disorder.

For $|K| \ll d$, the system is in the *Fermi glass* phase, i.e. Anderson localized (and many-body corrected) single particle states are occupied according to the Fermi–Dirac statistics [34]. The effect of disorder is to localize the fermions preferably into the deepest sites.

For repulsive and large composite interactions ($K > 0$ and $K \gg d$), the ground state is a Fermi MI phase and the composite fermions are pinned at large filling factors preferably into the deepest wells. At half-filling factor ($\rho_f = 1/2$), one expects the ground state to form a *checker board*, i.e. the lattice sites are alternatively empty and populated by one composite.

For large attractive composite interactions ($K < 0$ and $|K| \gg d$), the fermions form a *domain insulator* whose average position results from the competition between the random and the confining potential.

Finally, for intermediate values of K/d , with $K > 0$, *delocalized metallic* phases with enhanced persistent currents are possible [35]. Similarly, for attractive interactions ($K < 0$) and $|K| < d$ one expects a competition between pairing of fermions and disorder i.e. a *dirty superfluid* phase.

Further information is provided by numerical computations that we present now. We consider on-site random inhomogeneities for the bosons μ_i^b . We start from a non-disordered phase [$\Delta(t = 0) = 0$] and slowly increase the standard deviation of the disorder $\sqrt{\langle (\tilde{\mu}_i^b)^2 \rangle - \langle \tilde{\mu}_i^b \rangle^2} = \Delta(t)$ from 0 to its final value Δ .

We first study the transition from a (composite) *Fermi gas* in the absence of disorder (see figure 4(b)) to a (composite) *Fermi glass* (see figure 4(c)). Initially [$\Delta(t) = 0$], the composite fermions are delocalized although confined near the centre of the effective harmonic potential $[(\omega_f - \omega_b) \times l(i)^2]$. The local populations fluctuate around $\langle m_i \rangle \simeq 0.4$ with a standard deviation $\sqrt{\langle (m_i - \langle m_i \rangle)^2 \rangle} \simeq 0.43$. Increasing the amplitude of disorder, the fluctuations of m_i decrease as shown in figure 4(a). This indicates that the composites localize more and more in the lattice sites to form a Fermi glass. For $\Delta = 5 \times 10^{-4}$, the composite fermions

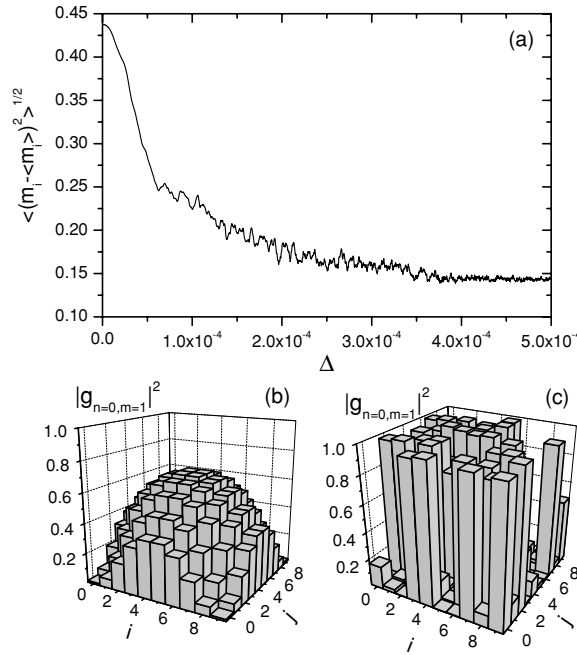


Figure 4. Dynamical crossover from the Fermi gas to the Fermi glass phases. The parameters are the same as in figure 2(c). (a) Variance of the number of fermions per lattice site as a function of the amplitude of the disorder Δ . (b) Probability of having one composite (one fermion and zero boson) at each lattice site for the M sites in the absence of disorder and (c) after ramping up adiabatically diagonal disorder with amplitude $\Delta = 5 \times 10^{-4}$.

are pinned in random sites as shown in figure 4(c). As expected, the N_f composite fermions populate the N_f sites with minimal $\tilde{\mu}_i^b$.

We now turn to the transition from a *Fermi insulator domain* phase (see figure 5(b)) to a *disordered insulating phase* while slowly increasing the amplitude of the disorder. For the Fermi insulator domain, the composite fermions are pinned near the centre of the harmonic trap and surrounded by a ring of delocalized fermions which results in finite fluctuations on the fermion occupation number ($\sqrt{\langle (m_i - \langle m_i \rangle)^2 \rangle} \simeq 0.35$). As shown in figure 5(a), while ramping up the amplitude of disorder, the fluctuations decrease down to $\sqrt{\langle (m_i - \langle m_i \rangle)^2 \rangle} \simeq 0.13$ for $\Delta > 10^{-4}$ showing that the composite fermions are pinned in different lattice sites. This can be seen in the plot the site population of the composite fermions presented in figure 5(c). Contrary to what happens for the transition from the Fermi gas to Fermi glass, the composites mostly populate the central part of the confining potential. This is because (i) the attractive interaction between composites is of the order of $K \simeq -1.4 \times 10^{-3}$ and competes with disorder ($\Delta = 3 \times 10^{-4}$) and (ii) because tunnelling is small ($d \simeq 8 \times 10^{-5}$) so the fermions can hardly move during the ramp of disorder.

4. The spin glass limit

4.1. From composite Hamiltonians to spin glass models

The second limit corresponds to a case where the interactions between fermions and bosons are of the order of, but slightly smaller than the interactions between the bosons ($\alpha \sim 1$ and $\alpha < 1$). As shown in figure 1, the effective interaction term $K_{i,j}$ has a zero at large

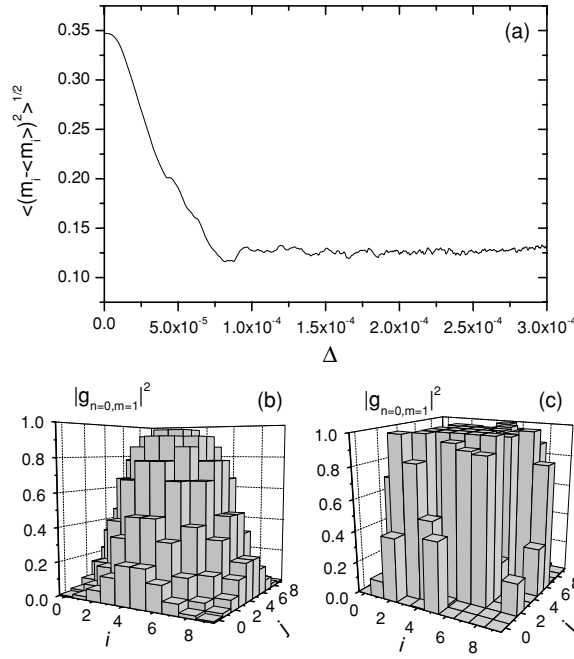


Figure 5. Dynamical crossover from the fermionic domain insulator to a disordered insulating phase. The parameters correspond to figure 2(d). (a) Variance of the number of fermions per lattice site as a function of the amplitude of the disorder. (b) Probability of having one composite (one fermion and zero boson) in each lattice site in the absence of disorder and (c) after ramping up adiabatically the disorder with amplitude $\Delta = 3 \times 10^{-4}$.

inhomogeneities $|\Delta_{i,j}^b|$ and varies strongly with $|\Delta_{i,j}^b|$ reaching both positive and negative values. Such a situation is accessible for ultracold atomic systems using a superlattice with a spatial period twice as large as the lattice spacing plus a random potential, both acting on the bosons. The interaction with this superlattice results in an alternatively positive and negative additional on-site energy of the bosons, whose amplitude is controlled by the intensity of the superlattice. In particular, one can set $|\Delta_{i,j}| \simeq \alpha$. An additional weak random potential introduces disorder.

Due to the random on-site effective energy $\bar{\mu}_i$, the effective tunnelling becomes non-resonant and can be neglected in first approximation while $K_{i,j}$ is random with a given average (eventually zero) and strong fluctuations from positive to negative values. The effective Hamiltonian (5) then reduces to

$$H_{\text{EA}} = \frac{1}{4} \sum_{\langle ij \rangle} K_{ij} s_i s_j + \frac{1}{2} \sum_i \bar{\mu}_i s_i, \quad (9)$$

where we have introduced $s_i = 2M_i - 1 = \pm 1$. Interpreting s_i as classical Ising spins¹⁰, this Hamiltonian is equivalent to the well-known Edwards–Anderson model [36]. This describes *spin glasses*, i.e., a Ising model with random positive (anti-ferromagnetic) or negative (ferromagnetic) exchange terms $K_{i,j}$. Our system however differs from the usual Edwards–Anderson spin glass model as (i) it has a random magnetic term $\bar{\mu}_i$ and (ii) the average magnetization per site $m = 2N_f/N - 1$ is fixed by the total number of fermions in the

¹⁰ Note that the spins commute in different sites $[s_i, s_j] = 0$.

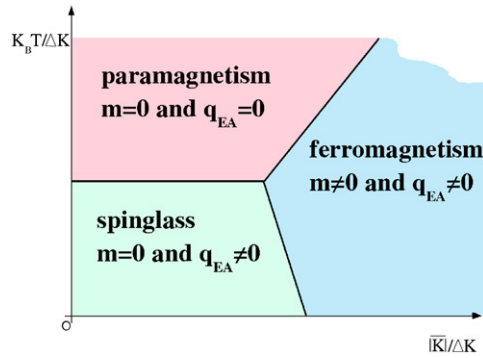


Figure 6. Schematic phase diagram of a spinglass.

lattice. It however shares basic characteristics with spin glasses as being a spin Hamiltonian with random spin exchange terms K_{ij} . In particular, this provides bond frustration, which is essential for the appearance of the spin glass phase and turns out to introduce severe difficulties for analytical and numerical analyses. We thus think that experiments with ultracold atoms can provide a useful *quantum simulator* to address challenging questions related to spin glasses such as the nature of the ordering of its ground- and possibly metastable states [4, 37, 38], broken symmetry and dynamics of spin glasses [5, 39].

In the following two sections, we outline some general properties of spin glasses and then we apply the *replica method* under the constraint of a fixed magnetization and argue that this preserves the occurrence of a symmetry breaking characteristics of spin glasses in the Mézard–Parisi theory [4].

4.2. Generalities on spin glasses

Consider a spin glass at finite temperature with a random exchange term K_{ij} with average \bar{K} and variance ΔK . The magnetization is characterized by two-order parameters: (i) $m = \overline{\langle s_i \rangle}$, the average magnetization per site and (ii) $q_{EA} = \overline{\langle s_i \rangle^2}$, the Edwards–Anderson parameter, where $\bar{\cdot}$ denotes the average over disorder while $\langle \cdot \rangle$ represents the thermodynamics average. It is clear that $m \neq 0$ signals a long-range magnetic order while $q_{EA} \neq 0$ signals a local magnetization that may vary from site to site and from one configuration of quenched disorder to another.

Earlier experimental studies have identified three magnetic phases as schematically represented in figure 6 [40]: (i) at high temperature and small average spin exchange \bar{K} , one finds a *paramagnetic phase* characterized by $m = q_{EA} = 0$. (ii) For $\bar{K} > 0$ and large, one has a *ferromagnet* with $m \neq 0$ and $q_{EA} \neq 0$. (iii) For weak \bar{K} and small temperatures, a *spin glass* phase appears with $m = 0$ but $q_{EA} \neq 0$. This signals that the local magnetization is frozen but that disorder prevents a long-range magnetic order.

As pointed out before, the physics of spin glasses still opens challenging questions. In particular, there are competing theories that predict different natures of the magnetic order.

The ‘droplet’ picture is a phenomenological theory based on numerical and scaling arguments. It predicts that there are two ground states related by spin-flip symmetry and that low-lying excitations are domains with fractal boundaries (the droplets) with all spins inverted compared to the ground state. This theory is supported by numerical computations and is believed to be valid in short-range spin glass models such as the Edwards–Anderson [36].

The Mézard–Parisi picture predicts a large number of low-energy states with very similar energies. This leads in particular to *disorder-induced quantum frustration*. This theory is a

mean field, based on the *replica method* which is a special trick introduced to compute the non-trivial average over disorder of the free energy functional. The Mézard–Parisi theory is formulated in long-range spin glasses such as the Sherrington–Kirkpatrick model

$$H_{S-K} = \frac{1}{4} \sum_{(ij)} K_{ij} s_i s_j + \frac{1}{2} \sum_i \bar{\mu}_i s_i \quad (10)$$

that differs from the Edwards–Anderson model (9) by the long-range spin exchange [(ij) denotes here the sum over *all* pairs of lattice sites, either neighbours or not)]. The applicability of the Mézard–Parisi picture to short-range spin glasses is still controversial.

4.3. The replica-symmetric solution for fixed magnetization

As the disorder is quenched, one must average over disorder the free energy density, $\bar{f} = -\overline{\ln Z}/k_B$ using the *replica trick*. In the following, we assume that the random variables K_{ij} and $\bar{\mu}_i$ are Gaussian distributed with average \bar{K} and h respectively and standard deviation ΔK and Δh respectively. We form n identical copies of the system (the *replicas*) and the average is calculated for an integer n and a finite number of spins N . Then, using the well-known formula $\ln x = \lim_{n \rightarrow 0} (x^n - 1)/n$, $\overline{\ln Z}$ is obtained from the analytic continuation of $\overline{Z^n}$ for $n \rightarrow 0$. Finally, we take the thermodynamic limit $N \rightarrow \infty$. Explicitly, $\overline{Z^n}$ is given by

$$\overline{Z^n} = \sum_{s_i^\alpha = \pm 1} \exp \left[-\overline{H[s_i^\alpha, n]} \right], \quad (11)$$

where $\overline{H[s_i^\alpha, n]}$ is the sum of n independent and identical spin Hamiltonians, averaged over the disorder, with Greek indices now numbering the n replicas. Computing the average over disorder leads to coupling between spin–spin interactions of different replicas.

After some analytics that are detailed in [26], one finally gets

$$\frac{\bar{f}_{SK}}{k_B T} = \frac{(K/k_B T)^2}{4} (1-q)^2 - \frac{(\Delta h/k_B T)^2}{2} + \int dz \frac{e^{-\frac{z^2}{2}}}{\sqrt{2\pi}} \ln \left[2 \cosh \frac{\sqrt{K^2 q + \Delta h^2} - \bar{h}}{k_B T} \right] \quad (12)$$

and

$$q = \int dz \frac{e^{-\frac{z^2}{2}}}{\sqrt{2\pi}} \tanh^2 \left(\frac{\sqrt{K^2 q + \Delta h^2} - \bar{h}}{k_B T} \right) \quad (13)$$

$$m = \int dz \frac{e^{-\frac{z^2}{2}}}{\sqrt{2\pi}} \tanh \left(\frac{\sqrt{K^2 q + \Delta h^2} - \bar{h}}{k_B T} \right). \quad (14)$$

These are the characteristic values of spinglasses that may be measured in the experimental realizations of the proposed systems.

Finally, a study of stability of the replica method as detailed in [26] shows that the magnetization constraint specific to our model would not change the occurrence of replica symmetry breaking, provided the Mézard–Parisi approach is valid in finite range spin glass models.

5. Conclusion

In this paper, we have reviewed our recent theoretical works on Fermi–Bose mixtures in disordered optical lattices. In the strongly correlated regime and under constraints that we

have discussed in detail, the physics of the mixture can be mapped into that of single-species Fermi composites. This is governed by a Fermi–Hubbard-like Hamiltonian with parameters that can be controlled with accuracy in state-of-the-art experiments on ultracold atoms.

We have shown that the presence of disorder (created by random on-site energies) introduces further control possibilities and induces an extraordinary rich quantum phase diagram. For the sake of conciseness, we have restricted our discussion to a particular regime that proves to be a case study (more details may be found in [26]). For a weak disorder, we have discussed the phase diagram which corresponds to the formation of Fermi glass, domain insulator, dirty superfluids and metallic phases. Numerical calculations support our discussion.

For larger amplitudes of disorder, we have shown that the Hamiltonian reduces to that of a spinglass, i.e. a spin system with random exchange terms. In our system, the fictitious spins are coded by the presence or the absence of particles in each lattice site. The physics of spinglasses is a challenging problem in statistical physics which is still unsolved. In particular, two theories are competing: the *droplet picture* and the *Mézard–Parisi picture*. These two theories lead to different predictions and even the nature of ordering in spinglasses is not known. On the one hand, the Mézard–Parisi picture, which is assumed to be valid for long-range spin exchange, predicts the existence of a huge number of quantum states with very similar energies that all contribute to the low-temperature physics of spinglasses. On the other hand, the droplet picture, which is believed to be valid for short spin exchange, assumes the existence of only two pure states connected by spin flip symmetry and excitations are domains of constant magnetization with fractal boundaries. As possible experimental realizations of spinglass systems with controllable parameters, mixtures of ultracold fermions and bosons may serve as *quantum simulators* to solve the controversy and shed new light on this extraordinary rich physics.

Acknowledgments

This work was supported by the Deutsche Forschungsgemeinschaft (SFB 407, SPP1116 436POL), the RTN Cold Quantum Gases, ESF PESC QUDEDIS, the Alexander von Humboldt Foundation and the Ministerio de Ciencia y Tecnología (BFM-2002-02588). JZ was supported by the Polish Government Research Funds under contract no. PBZ-MIN-008/P03/2003.

References

- [1] Anderson P W 1958 *Phys. Rev.* **109** 1492
- [2] Nagaoka Y and Fukuyama H (ed) 1982 *Anderson Localization (Springer Series in Solid State Sciences vol 39)* (Berlin: Springer)
- Ando T and Fukuyama H (ed) 1988 *Anderson Localization (Springer Proc. in Physics vol 28)* (Berlin: Springer)
- [3] Auerbach A 1994 *Interacting Electrons and Quantum magnetism* (New York: Springer)
- [4] Mézard M, Parisi G and Virasoro M A 1987 *Spin Glass and Beyond* (Singapore: World Scientific)
- [5] Sachdev S 1999 *Quantum Phase Transitions* (Cambridge: Cambridge University Press)
- [6] Efetov K 1997 *Supersymmetry in Disorder and Chaos* (Cambridge: Cambridge University Press)
- [7] Fisher M P A, Weichman P B, Grinstein G and Fisher D S 1989 *Phys. Rev. B* **40** 546
- [8] Shepelyansky D L 1994 *Phys. Rev. Lett.* **73** 2607
- [9] Aharony A and Stauffer D 1994 *Introduction to Percolation Theory* (London: Taylor and Francis)
- [10] Misguich G and Lhuillier C 2004 *Two-dimensional Quantum Anti-ferromagnets Frustrated Spin Systems* ed H T Diep (Singapore: World Scientific)
- [11] Damski B, Zakrzewski J, Santos L, Zoller P and Lewenstein M 2003 *Phys. Rev. Lett.* **91** 080403
- [12] Sanpera A, Kantian A, Sanchez-Palencia L, Zakrzewski J and Lewenstein M 2004 *Phys. Rev. Lett.* **93** 040401
- [13] Chu S 1998 Nobel lectures *Rev. Mod. Phys.* **70** 685

- Cohen-Tannoudji C 1998 Nobel lectures *Rev. Mod. Phys.* **70** 707
 Phillips W D 1998 Nobel lectures *Rev. Mod. Phys.* **70** 721
- [14] Cornell E A and Wieman C E 2002 *Rev. Mod. Phys.* **74** 875
 Ketterle W 2002 *Rev. Mod. Phys.* **74** 1131
- [15] Truscott A G, Strecker K E, McAlexander W I, Partridge G B and Hulet R G 2001 *Science* **291** 2570
 Köhl M, Moritz H, Stöferle T, Günter K and Esslinger T 2005 *Phys. Rev. Lett.* **94** 080403
- [16] Schreck F, Khaykovich L, Corwin K L, Ferrari G, Bourdel T, Cubizolles J and Salomon C 2001 *Phys. Rev. Lett.* **87** 080403
 Hadzibabic Z, Stan C A, Dieckmann K, Gupta S, Zwierlein M W, Görlitz A and Ketterle W 2002 *Phys. Rev. Lett.* **88** 160401
 Modugno G, Roati G, Riboli F, Ferlaino F, Brecha R J and Inguscio M 2002 *Science* **297** 2240
 Roati G, Riboli F, Modugno G and Inguscio M 2002 *Phys. Rev. Lett.* **89** 150403
- [17] For recent reviews, see 2002 *Nature* **416** 206–46
- [18] Inoué S, Andrews M R, Stenger J, Miesner H-J, Stamper-Kurn D M and Ketterle W 1998 *Nature* **392** 151
 Cornish S L, Claussen N R, Roberts J L, Cornell E A and Wieman C E 2000 *Phys. Rev. Lett.* **85** 1795
- [19] Grynberg G and Robilliard C 2000 *Phys. Rep.* **355** 335
- [20] Horak P, Courtois J-Y and Grynberg G 1998 *Phys. Rev. A* **58** 3953
- [21] Guidoni L, Triché C, Verkerk P and Grynberg G 1997 *Phys. Rev. Lett.* **79** 3363
 Guidoni L, Dépret B, Stefano A di and Verkerk P 1999 *Phys. Rev. A* **60** R4233
- [22] Sanchez-Palencia L and Santos L 2005 *Phys. Rev. A* **72** 053607
- [23] Clément D, Varón A F, Hugbart M, Retter J A, Bouyer P, Sanchez-Palencia L, Gangardt D, Shlyapnikov G V and Aspect A 2005 *Phys. Rev. Lett.* **95** 170409
- [24] Lye J E, Fallani L, Modugno M, Wiersma D, Fort C and Inguscio M 2005 *Phys. Rev. Lett.* **95** 070401
 Fort C, Fallani L, Guarrera V, Lye J, Modugno M, Wiersma D S and Inguscio M 2005 *Phys. Rev. Lett.* **95** 170410
- [25] Schulte T, Drenkelforth S, Kruse J, Ertmer W, Arlt J, Sacha K, Zakrzewski J and Lewenstein M 2005 *Phys. Rev. Lett.* **95** 170411
- [26] Ahufinger V, Sanchez-Palencia L, Kantian A, Sanpera A and Lewenstein M 2005 *Phys. Rev. A* **72** 063616
- [27] Wannier G H 1937 *Phys. Rev.* **52** 191
 Kittel C 1987 *Quantum Theory of Solids* (New York: Wiley)
- [28] Jaksch D, Bruder C, Cirac J I, Gardiner C W and Zoller P 1998 *Phys. Rev. Lett.* **81** 3108
- [29] Albus A, Illuminati F and Eisert J 2003 *Phys. Rev. A* **68** 023606
 Büchler H P and Blatter G 2003 *Phys. Rev. Lett.* **91** 130404
 Roth R and Burnett K 2004 *Phys. Rev. A* **69** 021601
 Roth R and Burnett K 2004 *J. Phys. B: At. Mol. Opt. Phys.* **37** 3893
 Illuminati F and Albus A 2004 *Phys. Rev. Lett.* **93** 090406
- [30] Lewenstein M, Santos L, Baranov M A and Fehrmann H 2004 *Phys. Rev. Lett.* **92** 050401
- [31] Cohen-Tannoudji C, Dupont-Roc J and Grynberg G 1992 *Atom-photon Interactions: Basic Processes and Applications* (New York: Wiley)
- [32] Mandel O, Greiner M, Widera A, Rom T, Hänsch T W and Bloch I 2003 *Phys. Rev. Lett.* **91** 010407
- [33] Abrahams E, Anderson P W, Licciardello D C and Ramakrishnan T V 1979 *Phys. Rev. Lett.* **42** 673
- [34] Freedman R and Hertz J A 1977 *Phys. Rev. B* **15** 2384
 Imry Y 1995 *Europhys. Lett.* **30** 405
 von Oppen F and Wettig T 1995 *Europhys. Lett.* **32** 741
 Jacoud Ph and Shepelyansky D L 1997 *Phys. Rev. Lett.* **78** 4986
- [35] Schmitteckert P, Jalabert R A, Weinmann D and Pichard J-L 1998 *Phys. Rev. Lett.* **81** 2308
 Benenti G, Waintal X and Pichard J-L 1999 *Phys. Rev. Lett.* **83** 1826
 Waintal X, Benenti G and Pichard J-L 2000 *Europhys. Lett.* **49** 466
 Gambeti-Césaire E, Weinmann D, Jalabert R A and Brune Ph 2002 *Europhys. Lett.* **60** 120
- [36] Edwards S F and Anderson P W 1975 *J. Phys. F: Met. Phys.* **5** 965
- [37] Fisher D S and Huse D A 1986 *Phys. Rev. Lett.* **56** 1601
 Bray A J and Moore M A 1987 *Phys. Rev. Lett.* **58** 57
 Fisher D S and Huse D A 1988 *Phys. Rev. B* **38** 373
 Fisher D S and Huse D A 1988 *Phys. Rev. B* **38** 386
- [38] Newman C M and Stein D L 2003 *J. Phys.: Condens. Matter* **15** R1319
- [39] Georges A, Parcollet O and Sachdev S 2001 *Phys. Rev. B* **63** 134406
- [40] Sherrington D 1998 *Preprint cond-mat/9806289*